

2022

## Perovskite solar cells

Liqiu Zheng Dr.

*Albany State University*, liqiu.zheng@asurams.edu

Tyler Hurst

*Albany State University*, t.hurst2120@gmail.com

Zhongrui Li

*University of Michigan*, zhongrui@umich.edu

Follow this and additional works at: <https://digitalcommons.gaacademy.org/gjs>



Part of the [Optics Commons](#), and the [Other Physics Commons](#)

---

### Recommended Citation

Zheng, Liqiu Dr.; Hurst, Tyler; and Li, Zhongrui (2022) "Perovskite solar cells," *Georgia Journal of Science*, Vol. 80, No. 2, Article 9.

Available at: <https://digitalcommons.gaacademy.org/gjs/vol80/iss2/9>

This Research Articles is brought to you for free and open access by Digital Commons @ the Georgia Academy of Science. It has been accepted for inclusion in Georgia Journal of Science by an authorized editor of Digital Commons @ the Georgia Academy of Science.

---

## Perovskite solar cells

### Acknowledgements

Acknowledgments: this work was supported by National Science Foundation (NSF) (Grant No.1700339)  
There is no conflict of interest to declare.

# Manganese Doped Perovskite CsPb<sub>0.9</sub>Mn<sub>0.1</sub>Br<sub>2</sub>I Solar Cells with Enhanced Stability and Reduced Toxicity

Liqu Zheng<sup>\*1</sup>, Tyler Hurst<sup>1</sup> and Zhongrui Li<sup>2</sup>

<sup>1</sup>Math, Computer Science and Physics Department, Albany State University, Albany, GA31707

<sup>2</sup> Electron Microbeam Analysis Laboratory, University of Michigan, Ann Arbor, MI48109

\*Corresponding Author: [Liqu.zheng@asurams.edu](mailto:Liqu.zheng@asurams.edu)

## ABSTRACT

The semiconductor perovskite CsPbBr<sub>2</sub>I was doped with Mn<sup>2+</sup> to modulate its optical and photovoltaic performance. The Mn<sup>2+</sup>-doped CsPb<sub>0.9</sub>Mn<sub>0.1</sub>Br<sub>2</sub>I exhibited improved crystalline quality. Ultraviolet and visible spectroscopy of Mn<sup>2+</sup>-doped CsPb<sub>0.9</sub>Mn<sub>0.1</sub>Br<sub>2</sub>I revealed enhanced absorption capacity. Although the efficiency was not as good as desired, the enhanced light absorption of CsPb<sub>0.9</sub>Mn<sub>0.1</sub>Br<sub>2</sub>I still boosted the photovoltaic performance when it was utilized as a light absorber in perovskite solar cells, along with a low-cost carbon electrode. Compared with its counterpart CsPbBr<sub>2</sub>I, the doped CsPb<sub>0.9</sub>Mn<sub>0.1</sub>Br<sub>2</sub>I based solar cells demonstrated long-term air stability. Not only long-lasting stability was achieved by doping with Mn<sup>2+</sup>, the toxicity was also lessened by replacing the amount of hazardous lead in perovskite with harmless manganese.

## KEYWORDS

Perovskite solar cells; Stability; Photovoltaic Performance; Light absorption; Toxicity.

## INTRODUCTION

Since organic-inorganic hybrid perovskite solar cells (SCs) hardly maintain device integrity and functionality when exposed to their surroundings, cesium (Cs) has been proposed to take the place of  $\text{CH}_3\text{NH}_3(\text{MA})$  to form all-inorganic halide perovskites  $\text{CsPbX}_3$  ( $\text{X} = \text{Cl}, \text{Br}, \text{I}$ ) to realize relatively long stability, albeit, far below the standard required by the Life Cycle Assessment for commercialized solar devices (Song et al 2007). Perovskites  $\text{CsPbX}_3$  have found widespread applications in photo-electrics devices (Hu 2017; Song 2015), due to the meritorious attributes like strong air and thermal stability, high light absorption coefficients, and outstanding charge transport with a reasonably long exciton diffusion length. In addition, the low temperature and low processing cost allows for roll-to-roll manufacturing with flexible substrates (Li et al 2017). However, some challenges still persist. A wide bandgap of 2.3 eV for  $\text{CsPbBr}_3$  limits its absorption, thereby causing an optimal performance of 10.6% (Zheng et al 2021). Despite having an ideal bandgap of 1.73 eV,  $\alpha\text{-CsPbI}_3$  (cubic phase) is merely stable at high temperatures ( $>300^\circ\text{C}$ ), easily turning into the undesirable  $\delta\text{-CsPbI}_3$  (non-perovskite phase) under ambient conditions (Eperon et al 2015). The unfavorable structural phase transition causes photo- and thermal-instability of perovskite solar cells which demands tremendous efforts to address this crucial issue. Meanwhile, it is hard to fabricate  $\alpha\text{-CsPbI}_3$  based SCs under routine conditions. Moreover, the toxicity of lead-based compounds poses an environmental hazard for outdoor applications. The existing issues necessitate the pursuit of alternatives beyond  $\text{MAPbI}_3$ . Therefore, identifying the right ingredients for perovskites to achieve ideal photoelectronic properties and strengthen stability, at a lessened cost to the environment, has proven to be a compelling challenge.

Mixed-halide based perovskites are more appealing in photovoltaic cells compared to the pure halide-based counterparts due to their wider optical tenability and band-gaps. Partially substituting iodide (I) with bromide (Br) (Yan 2018; Guo 2019) to tune the tolerance factor of perovskite structure, has been attempted. For instance,  $\text{CsPbBr}_2\text{I}$  (with a band gap  $\approx 2.05$  eV) has been reported with the best efficiency of 9.8% to date (Guo et al 2019). The inclusion of bromide favors the stabilization of the perovskite phase at lower temperatures, although it implies a widening of the bandgap as a consequence of the substitution of iodide with a more electronegative halide. In spite of the relatively lower efficiency,  $\text{CsPbBr}_2\text{I}$ , is more stable to environmental exposure than the other mixed Br/I

ratio perovskites such as CsPbI<sub>3</sub> and CsPbI<sub>2</sub>Br, at the same time, possessing a broader absorption range than that of CsPbBr<sub>3</sub>.

In order to fine-tune the electronic and optical properties of II-VI semiconductors, the incorporation of impurity ions has been demonstrably effective (He 2017; Peng 2012). Due to the strong exchange interactions of the  $\frac{5}{2}$  Mn<sup>2+</sup> spin with conduction and valence band carriers, along with a new emission channel at ~2.15eV (an internal <sup>4</sup>T<sub>1</sub> to <sup>6</sup>A<sub>1</sub> transition), after introducing Mn<sup>2+</sup>, the optical, electronic and magnetic structure of the host semiconductor materials could be drastically altered to impart desirable properties which allow for widespread applications in high efficiency solar cells, color-tunable light emitting diodes and lasers. In this work, for the first time with the hope of enhanced efficiency, along with better stability and reduced toxicity, the incorporation of dopant manganese into CsPbBr<sub>2</sub>I, will be investigated and compared. It turns out the strengthened stability and the reduced toxicity could be realized by manganese doping into CsPbBr<sub>2</sub>I, notwithstanding sacrificing efficiency. In spite of the compromised efficiency, our comparative study still sheds light on how dopants affect the photovoltaic performance of perovskites, providing insights into developing a large variety of semiconductors for enhanced light absorption, tunable color emission or other practical photovoltaic applications.

### EXPERIMENTAL DETAILS

Glasses coated with fluorine-doped tin oxide (FTO) were washed sequentially with detergent, ethanol, and acetone with ultrasonication for 20 min each. They were dried by nitrogen and treated by plasma for 20 min, respectively. TiO<sub>2</sub> layer was first deposited on FTO substrate by spin-coating an ethanol solution of titanium isopropoxide and diethanol amine at 6000 rpm for 20 s, and then the FTO/TiO<sub>2</sub> substrate was annealed at 450 °C for 2 h in the air. The perovskite films of CsPb<sub>0.9</sub>Mn<sub>0.1</sub>Br<sub>2</sub>I and CsPbBr<sub>2</sub>I as the control were synthesized through a two-step solution method in the air without any control of humidity. For the synthesis of CsPb<sub>0.9</sub>Mn<sub>0.1</sub>Br<sub>2</sub>I films, 0.9 mmol PbBr<sub>2</sub> and 0.1 mmol MnBr<sub>2</sub> were dissolved in a mixture of solvents with dimethyl sulfoxide (DMSO)/DMF ratio at 2:3 (for improving the crystallization, exhibiting the least number of defects, and forming final pin-hole free films (Zheng et al 2021)) to yield a 1.0 M solution under stirring at 80 °C for 30 min. Similarly, for CsPbBr<sub>2</sub>I, 1.0 mmol PbBr<sub>2</sub> was dissolved in a mixture of solvents with dimethyl sulfoxide (DMSO) and DMF to yield a 1.0 M solution under stirring at 80 °C for 30 min. Then, the mixture solution was deposited on the FTO/TiO<sub>2</sub> substrates by spin-

coating at 2000 rpm for 30 s, and then dried at 80 °C for 30 min. Then, the obtained substrates were dipped separately into two beakers with a methanol solution of 15 mg/mL CsI for 10 min, and then washed with isopropoxide, dried by nitrogen, and heated at 350 °C for 45 s in the air. The obtained perovskite films of CsPb<sub>0.9</sub>Mn<sub>0.1</sub>Br<sub>2</sub>I and CsPbBr<sub>2</sub>I were transferred into the glovebox. Finally, conductive carbon ink was doctor-blade coated into carbon electrodes and then heated at 80 °C for 60 min.

X-ray diffraction patterns were collected on a Rigaku Ultima IV diffractometer in a grazing incident mode with an incident angle of 0.5 degree. Cu *K-alpha* line (wavelength=0.15418 nm) was utilized as a light source. UV-vis optical absorption spectra were recorded in an absorbance mode on a Varian Cary Bio 50 UV-visible spectrophotometer. The current density–voltage characteristic curves were recorded under AM1.5 illumination (100 mW/cm<sup>2</sup>) of a small-area class-B solar simulator (PV Measurements, Inc.) by a Keithley 2450 source meter, in which current was continuously measured as a function of voltage with a step of 0.02 V.

## RESULTS AND DISCUSSIONS

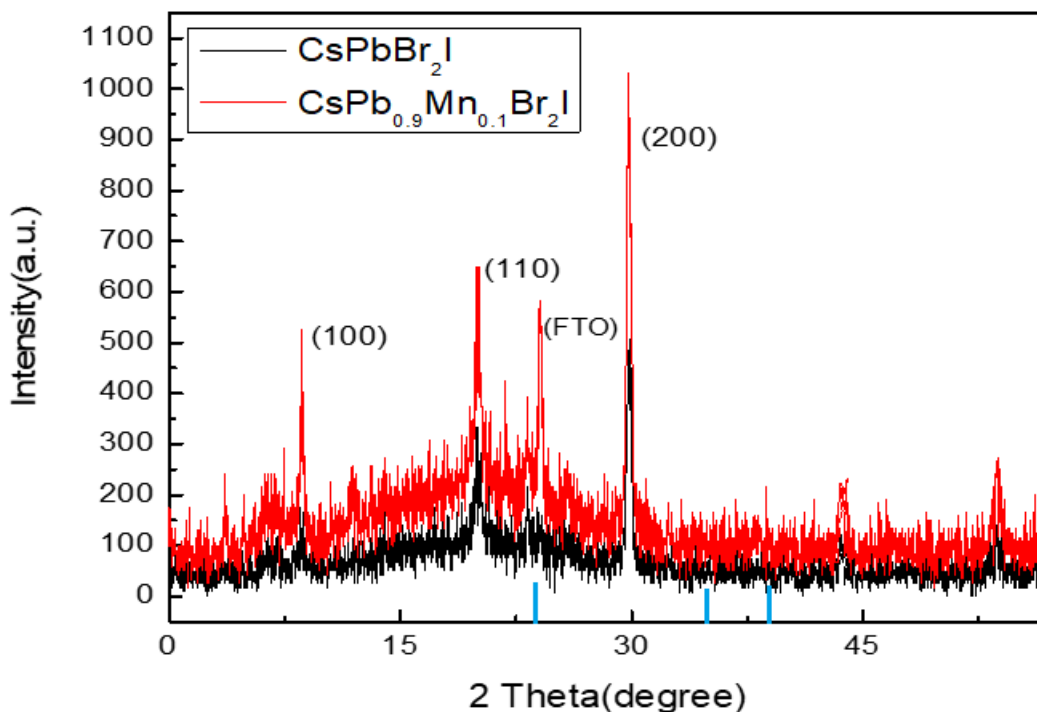


**Figure 1: X-ray Diffraction Patterns**

The crystallinities of CsPb<sub>0.9</sub>Mn<sub>0.1</sub>Br<sub>2</sub>I and CsPbBr<sub>2</sub>I (as the control) were examined by X-ray diffraction (XRD) patterns as shown in Figure 1. The thickness and uniformity of the films play a part in XRD pattern. Additionally, Pb absorbs more X-rays than Mn does such that the penetration depth of X-rays is shallower in the Pb film than that in the Mn-doped film, as a result, only one peak from the FTO substrate is visible in Mn-doped films, as disclosed in Figure 1. (Note since XRD of FTO is viewed as the standard background, only the positions of 3 peaks between 20°-50° were marked as blue bars in the graph). Identifiable XRD peaks could be indexed to the standard patterns of CsPbBr<sub>2</sub>I in the cubic phase of perovskite (Ma 2016; Lau 2016). After the incorporation of Mn dopants, no additional peaks could be detected, indicating that upon Mn-doping, no phase separation/alteration occurred in cube-shaped orthorhombic CsPbBr<sub>2</sub>I structures. XRD results amply suggest that Mn<sup>2+</sup> replaced Pb<sup>2+</sup>. No new diffraction peaks showed up suggesting that the perovskite structure was well reserved. The changes in diffraction intensity are due to the replacement of Pb by Mn. As the diffraction intensity can be expressed in Eq. (1) as the structure factor times its conjugate:

$$I \sim F_{hkl}^* \cdot F_{hkl}, \quad (1)$$

In which  $F_{hkl}$  is the vector sum of waves scattered by all atoms within the unit cell and (h,k,l) are the Miller indices in the real-space plane (Cowley 1992).

The structure factor as expressed in Eq. (2)

$$F_{hkl} = \sum_{j=1}^N f_j e^{[-2\pi i(hx_j + ky_j + \ell z_j)]}, \quad (2)$$

is proportional to the atomic scattering factor ( $f_j$ , charge of the element in the  $j$ -th unit cell) (Li 2020) in which  $x_j, y_j, z_j$  are the positional coordinates of the  $j$ -th atom, and  $N$  refers to all atoms in the unit cell. However, the peaks intensities of (100) and (200) are greatly strengthened, suggesting the crystal domains are highly oriented along the (100) planes. The better crystallinity for  $\text{CsPb}_{0.9}\text{Mn}_{0.1}\text{Br}_2\text{I}$  is reflected by the peaks of the XRD patterns for relatively large crystal sizes, which is in good agreement with results reported by Bai et al. Their interpretation is that the  $\text{Mn}^{2+}$ -doped  $\text{CsPbBr}_2\text{I}$  perovskite solar cells (PSCs) with larger microcrystalline grains and fewer grain boundaries are controlled by the doping of  $\text{Mn}^{2+}$  ions (Bai et al 2018). The enhanced crystallinity in Mn-doped perovskite film resulted from the removal some of preexisting structural defects by introducing Mn ions, leading to continuous charge-transport channels and thus enabling the high mobility of photogenerated carriers. In the halide perovskite crystals, dopant  $\text{Mn}^{2+}$  was substituted for  $\text{Pb}^{2+}$ . Because  $\text{Mn}^{2+}$  is smaller than  $\text{Pb}^{2+}$  and both are isovalent, no shifting of the diffraction peaks to higher  $2\theta$ -values was observed which confirms that smaller  $\text{Mn}^{2+}$  ions replaced isovalent  $\text{Pb}^{2+}$  ions. Thus, it is predominantly a case of substitutional doping.

Apart from the impact on interplanar distance in the crystal, the substitutional replacement of Pb also affected the optical properties of the perovskite crystals. As shown in Figure 2, ultraviolet-visible absorption spectra revealed the absorption capacity of  $\text{CsPb}_{0.9}\text{Mn}_{0.1}\text{Br}_2\text{I}$  and  $\text{CsPbBr}_2\text{I}$ . The absorption onset at approximately 600 nm of  $\text{CsPbBr}_2\text{I}$ , corresponds to the bandgap of  $\sim 2.05$  eV calculated from the Tauc Plots, which is consistent with the reported values for solution-derived  $\text{CsPbBr}_2\text{I}$  films (Zhang et al 2019). A slight red shift of the absorbing peak from  $\text{CsPbBr}_2\text{I}$  to  $\text{CsPb}_{0.9}\text{Mn}_{0.1}\text{Br}_2\text{I}$  was observed. Moreover, the absorbance intensity of Mn-doped perovskite  $\text{CsPb}_{0.9}\text{Mn}_{0.1}\text{Br}_2\text{I}$  became much stronger over the absorbing range, which can be attributed to the extra channel at 590 nm due to transfer of exciton energy from the host to d-states of Mn. This transition is both spin and orbit forbidden, leading to a very long lifetime in the range of several

hundreds of microseconds, which is advantageous to boost the efficiency of solar cells due to the long-lived charge carriers (Beaulac 2008; Vlaskin 2010). Since doping of manganese also changes multiphoton absorption (MPA) properties of host perovskites by forming defect levels in the bandgap, high quantum yield could be achieved due to an extremely efficient energy/charge transfer (Liang et al 2018). The photo-excited electron-hole pair of the perovskite follows non-radiative recombination, transferring energy from the host perovskites to Mn to excite the Mn<sup>2+</sup> ground state <sup>6</sup>A<sub>1</sub> to its excited <sup>4</sup>T<sub>1</sub> state. This energy transfer process should be very rapid and is typically expected to occur within a timescale of a few femtoseconds. For the charge transfer, the photoexcited hole can quickly relocate to the Mn sites resulting in a transient Mn<sup>3+</sup> nature. Due to a ground state of <sup>5</sup>E in the Mn<sup>3+</sup> ions and the first excited state of <sup>5</sup>T<sub>2</sub>, spin is conserved and an allowed absorption from <sup>5</sup>E to <sup>5</sup>T<sub>2</sub> state occurs, wherein the photo-excited electron is later captured to reach a more stable Mn<sup>2+</sup> state (Su et al 2021). The introduction of the intermediate band in the substitutional Mn-doped CsPbBr<sub>2</sub>I enables triple-photon transitions, ensuring higher quantum yield. The plots of UV-Vis absorption spectra were transformed to Tauc plots of  $(Ah\nu)^2$  vs.  $h\nu$  curves as shown in Figure 3, demonstrably revealing the bandgaps of perovskite films. The bandgap of CsPbBr<sub>2</sub>I with 2.05 eV shifted slightly to 2.02 eV of CsPb<sub>0.9</sub>Mn<sub>0.1</sub>Br<sub>2</sub>I, which is beneficial to the light harvesting.

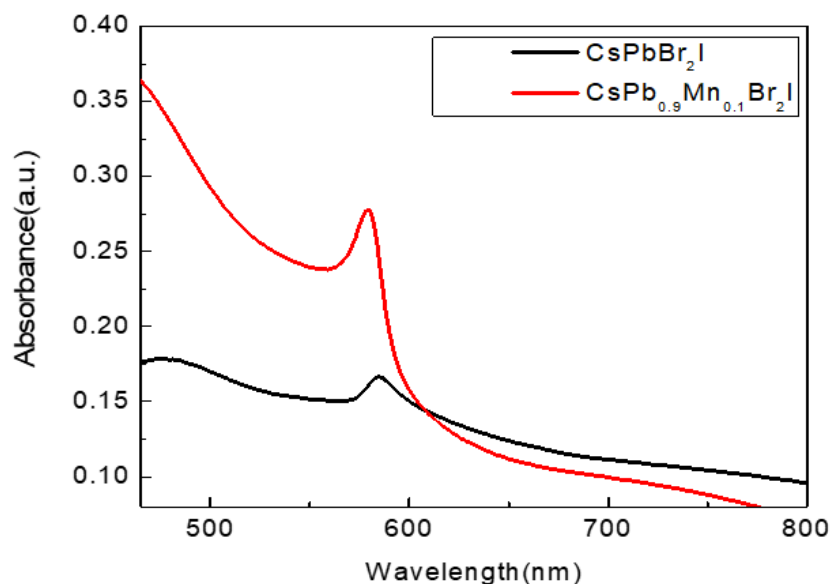


**Figure 2.** the UV-Vis Spectra for CsPb<sub>0.9</sub>Mn<sub>0.1</sub>Br<sub>2</sub>I and CsPbBr<sub>2</sub>I

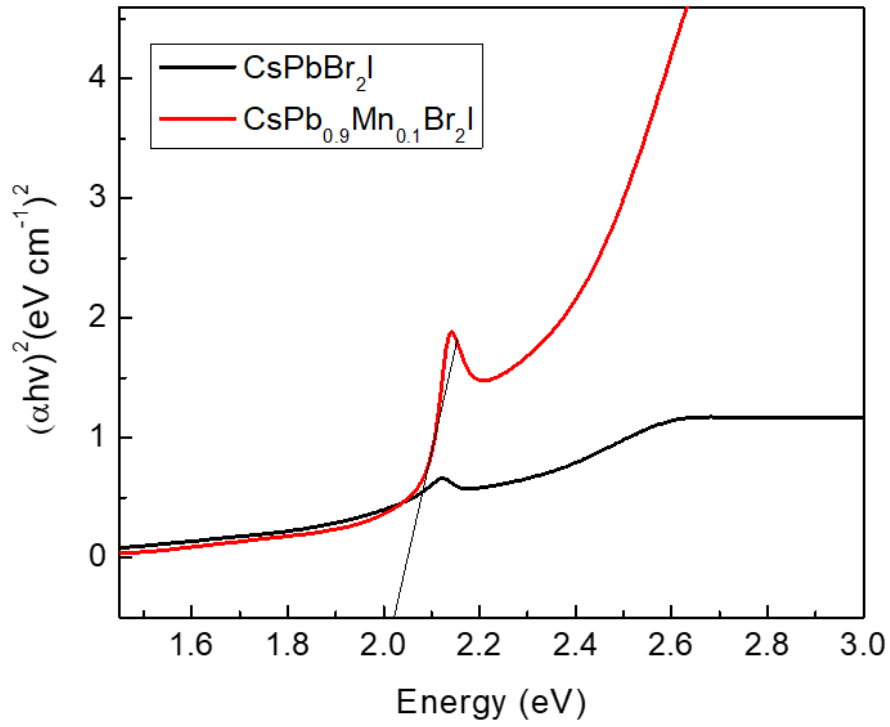
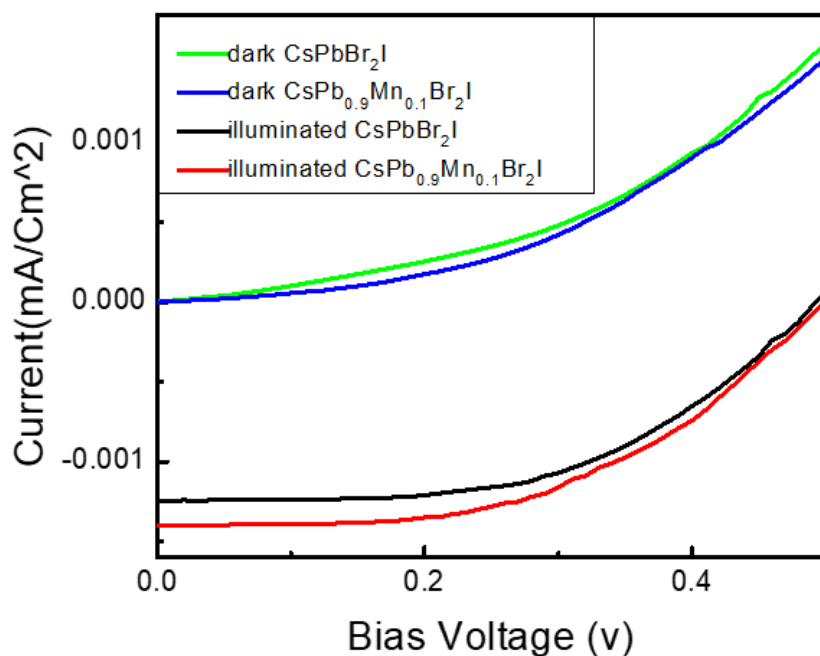
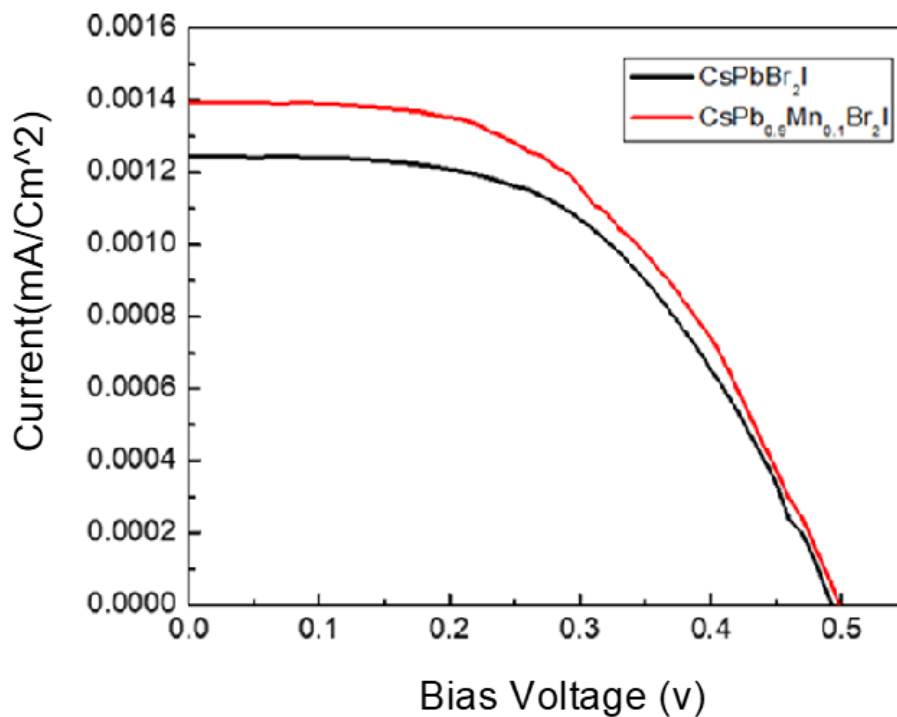


**Figure 3. Tauc Plots.**



a) IV curves for dark and under illumination



b) illuminated curves flipped into the first quadrant

**Figure 4. a) both dark and illuminated curves  
b) I-V curves in the first quadrant.**

Photovoltaic effects of the constructed solar cells were evaluated by the photo current–voltage curves in the dark and under 1 sun illumination as portrayed in Figure 4(a). The dark curves of both samples displayed the nonlinear rectifying characteristics which is a typical diode-like behavior for solar cells. To evaluate the photovoltaic performance, the illuminated curves were flipped into the first quadrant as seen in Figure 4(b). Under the identical conditions, the power conversion efficiency (PCE) of CsPb<sub>0.9</sub>Mn<sub>0.1</sub>Br<sub>2</sub>I based solar cells was 3.72%, outperforming that of the undoped CsPbBr<sub>2</sub>I counterpart (with the PCE of 3.19%). The short circuit current density  $J_{sc}$  of CsPb<sub>0.9</sub>Mn<sub>0.1</sub>Br<sub>2</sub>I is 14 mA/cm<sup>2</sup>, higher than that of CsPbBr<sub>2</sub>I with 12.3 mA/cm<sup>2</sup> although they have comparable open circuit voltage ( $V_{oc}$ ), which approximates to 0.5 V. The  $V_{oc}$  of CsPbBr<sub>2</sub>I is slightly below that of CsPb<sub>0.9</sub>Mn<sub>0.1</sub>Br<sub>2</sub>I, as a result of no dramatic bandgap change introduced by manganese dopants. It is particularly the case that the compatible band alignment and efficient host exciton energy transfer to Mn states are more favorable in perovskite hosts. The better photovoltaic performance of CsPb<sub>0.9</sub>Mn<sub>0.1</sub>Br<sub>2</sub>I is ascribed to multi-photon transitions introduced by the intermediate band in the substitutional Mn-doped CsPbBr<sub>2</sub>I. On the other hand, the interstitial Mn-doped CsPbBr<sub>2</sub>I, if any, is n-type doping, which improves the conductivity of CsPb<sub>0.9</sub>Mn<sub>0.1</sub>Br<sub>2</sub>I when compared to that of CsPbBr<sub>2</sub>I. Along with better crystallinity, the improved conductivity facilitated the photo-carriers transport and extraction, possibly improving the device performance of perovskite solar cells.

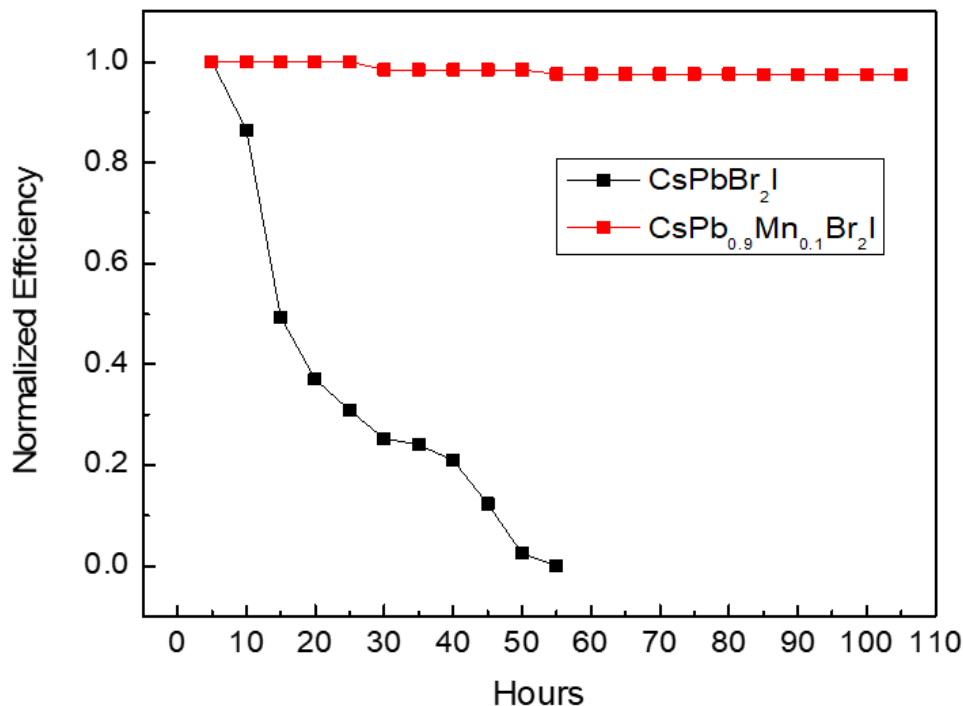


**Figure 5. Assessment of stability of constructed solar cells**

Doping manganese into perovskites impacts the crystallinity as revealed by XRD, which leads to much better stability. As shown in Figure 5, after 10 hours, the PCE of CsPbBr<sub>2</sub>I drastically decreased. After the first two days, the cells lost their functionality completely. However, the PCE of CsPb<sub>0.9</sub>Mn<sub>0.1</sub>Br<sub>2</sub>I retained its 96% efficiency for more than 100 hours under the ambient conditions in spite of a slight loss in the PCE. The relatively long-lasting stability is attributed to the enhanced thermodynamic stability of the substitutional and interstitial Mn-doped CsPb<sub>0.9</sub>Mn<sub>0.1</sub>Br<sub>2</sub>I in terms of binding energy. Specifically, the Mn<sup>2+</sup> ion ( $\approx 0.97 \text{ \AA}$ ) possesses a smaller radius than that of the Pb<sup>2+</sup> ion ( $\approx 1.33 \text{ \AA}$ ), leading to the contraction of the BX<sub>6</sub> (B = Pb or Mn; X = I or Br) octahedral volume and the changes of chemical bonding properties. Phase stability of perovskites is determined by the volumetric ratios between BX<sub>6</sub> octahedra and Cs cation. The contraction of the BX<sub>6</sub> octahedra leads to much better holding of the BX<sub>6</sub> octahedra in position by the Cs cations in the perovskite structure, which is more energetically favorable (Cowley 1992; Beaulac 2018), resulting in the enhancement of phase stability of CsPb<sub>0.9</sub>Mn<sub>0.1</sub>Br<sub>2</sub>I films. Liang et al (Liang et al 2018)

demonstrated that the maximum PCE of  $\text{Mn}^{2+}$ -doped perovskite solar cells can reach 7.36%, much better than the pure thin films. The PCE of the perovskite solar cells fabricated with  $\text{CsPb}_{0.995}\text{Mn}_{0.005}\text{I}_{1.01}\text{Br}_{1.99}$  only slightly declines to 92% of their pristine value after operating above 300 h. Moreover, the excess  $\text{Mn}^{2+}$  ions, if any, gathered at grain boundary surfaces can enhance the hole extraction efficiency by decreasing recombination loss. As a result, the optimized device using the doped  $\text{CsPbI}_2\text{Br}$  film achieves a stabilized efficiency as high as 15.52%, in which the device maintains 97% of their pristine value after 3 months under operating conditions (temperature of 25 °C and relative humidity of (25–35%) (Mali et al 2021). In a nutshell, the introduction of manganese into perovskite made a significant difference on the stability, which is a crucial step toward the outdoor applications for perovskite solar cells. It is noteworthy that innocuous dopant manganese substituting for lead to reduce the toxicity of lead-based perovskites, is another significant step toward real world applications of all-inorganic perovskite solar cells.

Due to the uniqueness of manganese as dopants, enormous efforts have been devoted to looking into  $\text{Mn}^{2+}$ -doped perovskite solar cells with long-lived charge carriers for better efficiency and long-term stability (Guria 2017; Deng 2021). More significantly, dopant manganese in II–VI materials finds even more extensive applications in the material fields (Liu et al 2017). Incorporation of manganese into the crystal lattice not only introduces a new emission channel at  $\sim 2.15$  eV, due to an internal  ${}^4\text{T}_1$  to  ${}^6\text{A}_1$  transition of the Mn ion, which is largely insensitive to the exact physical and electronic structure of the host materials, but also imparts paramagnetism to II–VI materials, because of strong exchange interactions of the  $5/2$   $\text{Mn}^{2+}$  spin with conduction- and valence-band carriers. The dopant of manganese creates electronic states in the midgap regions thus altering the charge separation and recombination dynamics, and possibly tuning the optical and electronic properties of semiconductor nanocrystals by controlling concentration of dopants. For instance, doping of  $\text{Mn}^{2+}$  ions in semiconductor crystals is known to achieve emission wavelengths in the range of 585–600 nm, which is an additional advantage for bioimaging applications compared to their blue or green counterparts (Adhikari et al 2017). More interestingly, doping of  $\text{Mn}^{2+}$  ions in host materials can also lead to longer lifetimes up to microseconds, enabling the temporal discrimination of the signal from the autofluorescence background, and has become the most favorable candidates for multiphoton fluorescent probes in biomedical applications (De 2017; Lin 2017).

## CONCLUSIONS

In order to improve optical and electronic performance, the semiconductor perovskite CsPb<sub>0.9</sub>Mn<sub>0.1</sub>Br<sub>2</sub>I was doped with Mn<sup>2+</sup>. As Mn<sup>2+</sup> ions reside at the Pb<sup>2+</sup> positions in the crystal lattice of CsPb<sub>0.9</sub>Mn<sub>0.1</sub>Br<sub>2</sub>I, the uniqueness of this dopant offers a long life-time spin polarized d-d emission. In the meantime, innocuous dopant manganese could reduce the toxicity of lead-based perovskites. X-ray diffraction revealed the quality crystalline of the Mn<sup>2+</sup>-doped CsPbBr<sub>2</sub>I, while ultra-violet and visible spectroscopy disclosed the enhanced absorption capacity, which boosted the photovoltaic performance when it was constructed as a light absorber in a perovskite solar cell. Additional investigation needs to be done to optimize the doping level and each layer to further boost the efficiency because it was relatively mediocre when compared with its other counterparts. More importantly, CsPb<sub>0.9</sub>Mn<sub>0.1</sub>Br<sub>2</sub>I demonstrated long-term air stability, compared with its counterpart CsPbBr<sub>2</sub>I. Not only was long lasting stability achieved by doping Mn<sup>2+</sup> but toxicity was also lessened by replacing the amount of hazardous lead in perovskite with harmless manganese. Attaining long-lasting stability and lessened toxicity is a critical step toward outdoor practical applications of perovskite solar cells.

## ACKNOWLEDGMENTS

This work was supported by National Science Foundation (NSF) (Grant No.1700339)

There is no conflict of interest to declare.

## REFERENCES

- Adhikari S. D., S. K. Dutta, A. Dutta, A. K. Guria, and N. Pradhan, "Chemically Tailoring the Dopant Emission in Manganese-Doped CsPbCl<sub>3</sub> Perovskite Nanocrystals", *Angew. Chem. Int. Ed.* 2017, 56, 8746–8750, DOI: 10.1002/anie.201703863.
- Bai D.L., J.R. Zhang, Z.W. Jin, H. Bian, K. Wang, H.R. Wang, L. Liang, Q. Wang, and S.Z. Liu, "Interstitial Mn<sup>2+</sup>-Driven High-Aspect-Ratio Grain Growth for Low-Trap-Density Microcrystalline Films for Record Efficiency CsPbI<sub>2</sub>Br Solar Cells", *ACS Energy Lett.* 2018, 3, 4, 970–978, DOI:10.1021/acsenergylett.8b00270.

- Beaulac R., P. I. Archer, X. Y. Liu, S. Lee, G. M. Salley, M. Dobrowolska, J. K. Furdyna, and D. R. Gamelin, "Spin-Polarizable Excitonic Luminescence in Colloidal Mn<sup>2+</sup>-doped CdSe Quantum Dots", *Nano Lett.* 2008, 8,1197–1201, DOI:10.1021/nl080195p.
- Cowley, J. M. (1992). *Electron Diffraction Techniques Vol 1*. Oxford Science. ISBN 9780198555582.
- De A., N. Mondal and A. Samanta, "Luminescence tuning and exciton dynamics of Mn-doped CsPbCl<sub>3</sub> nanocrystals", *Nanoscale*, 2017, 9, 16722–16727, DOI: 10.1039/c7nr06745c.
- Deng L.L., H.J. Yang, R.H. Pan, H.M. Yu, J.P. Li, L. Xu and K. Wang, "Achieving 20% photovoltaic efficiency by manganese doped methylammonium lead halide perovskites", *Journal of Energy Chemistry*, 60 (2021) 376–383, DOI: 10.1016/j.jechem.2021.01.028.
- Eperon G. E., G. M. Paterno, R. J. Sutton, A. Zampetti, A. A. Haghighirad, F. Cacialli and H. J. Snaith, "Inorganic cesium lead iodide perovskite solar cells", *J. Mater. Chem. A*, 2015, 3, 19688–19695, DOI:10.1039/C5TA06398A.
- Guo Y., X. Yin, J. Liu and W. Que, "Highly efficient CsPbIBr<sub>2</sub> perovskite solar cells with efficiency over 9.8% fabricated using a preheating-assisted spin-coating method", *J. Mater. Chem. A*, 2019, 7,1900. DOI:10.1039/C9TA03336J.
- Guria A. K., S. K. Dutta, S. D. Adhikari, and N. Pradhan, "Doping Mn<sup>2+</sup> in Lead Halide Perovskite Nanocrystals: Successes and Challenges", *ACS Energy Lett.* 2017, 2, 1014–1021, DOI: 10.1021/acsenergylett.7b00177.
- He T.C., J.Z. Li, C. Ren, S.Y. Xiao, Y.W. Li, R. Chen, and X.D. Lin, "Strong two-photon absorption of Mn-doped CsPbCl<sub>3</sub> perovskite nanocrystals", *Appl. Phys. Lett.* 2017,111, 211105, DOI:10.1063/1.5008437.
- Hu Z.P., Z.Z. Liu, Y. Bian, D.J. Liu, X.S. Tang, W. Hu, Z.G. Zang, M. Zhou, L.D. Sun, J.X. Tang, Y.Q. Li, J. Du and Y.X. Leng, "Robust Cesium Lead Halide Perovskite Microcubes for Frequency Upconversion Lasing", *Adv. Optical Mater.* 2017, 5, 1700419, DOI: 10.1002/adom.201700419.
- Lau C. F. J., X. F. Deng, Q. S. Ma, J. H. Zheng, J. S. Yun, M. A. Green, S. J. Huang, A. W. Y. Ho-Baillie, "CsPbIBr<sub>2</sub> Perovskite Solar Cell by Spray-Assisted Deposition", *ACS Energy Lett.* 2016,1, 573, DOI:10.1021/acsenergylett.6b00341.

- Li Y., Z.-F. Shi, S. Li, L.-Z. Lei, H.-F. Ji, D.Wu, T.-T. Xu, Y.-T. Tian and X.-J. Li, "High-performance perovskite photodetectors based on solution-processed all-inorganic CsPbBr<sub>3</sub> thin films", *J. Mater. Chem. C*, 2017,5, 8355-8360, DOI:10.1039/C7TC02137B.
- Li Z.R., "Advances in X-ray Absorption Fine Structure Analysis (Materials Science)", 2020, ISBN-13: 978-1925823882.
- Liang J., Z.H. Liu, L.B. Qiu, Z. Hawash, L.Q. Meng, Z.F. Wu, Y. Jiang, L. K. Ono, and Y.B. Qi, "Enhancing Optical, Electronic, Crystalline, and Morphological Properties of Cesium Lead Halide by Mn Substitution for High-Stability All-Inorganic Perovskite Solar Cells with Carbon Electrodes", *Adv. Energy Mater.* 2018, 8, 1800504. DOI: 10.1002/aenm.201800504.
- Lin C.C., K.Y. Xu, D. Wang & A. Meijerink, "Luminescent manganese-doped CsPbCl<sub>3</sub> perovskite quantum dots", *Sci. Rep.*, 2017, 7:45906, DOI: 10.1038/srep45906.
- Liu H.W., Z.N. Wu, J.R. Shao, D. Yao, H. Gao, Y. Liu, W.L. Yu, H. Zhang, and B. Yang, "CsPb<sub>x</sub>Mn<sub>1-x</sub>Cl<sub>3</sub> Perovskite Quantum Dots with High Mn Substitution Ratio", *ACS Nano* 2017, 11, 2239–2247, *ACS Nano* 2017, 11, 2239–2247, DOI:10.1021/acsnano.6b08747.
- Ma Q. S., S. J. Huang, X. M. Wen, M. A. Green, A. W. Y. Ho-Baillie, "Hole Transport Layer Free Inorganic CsPbI<sub>2</sub>Br<sub>2</sub> Perovskite Solar Cell by Dual Source Thermal Evaporation" *Adv. Energy Mater.* 2016, 6, 1502202, DOI: 10.1002/aenm.201502202.
- Mali S.S., J. V. Patil and C. K. Hong, "Simultaneous Improved Performance and Thermal Stability of Planar Metal Ion Incorporated CsPbI<sub>2</sub>Br All-Inorganic Perovskite Solar Cells Based on MgZnO Nanocrystalline Electron Transporting Layer", *Advanced Energy Materials*, 2020, 10 (3), 1902708, DOI:10.1002/aenm.201902708.
- Peng X., J. Li, Y. Yang, H. Gong, F. Nan, L. Zhou, X. Yu, Z. Hao, and Q. Wang, "Tunable nonlinear optical absorption in semiconductor nanocrystals doped with transition metal ions", *J. Appl. Phys.* 2012,112, 074305, DOI: 10.1063/1.4754856.
- Song J.Z., J.H. Li, X.M. Li, L.M. Xu, Y.H. Dong and H.B. Zeng, "Quantum Dot Light-Emitting Diodes Based on Inorganic Perovskite Cesium Lead Halides", *Adv. Mater.* 2015, 27, 7162–7167, DOI: 10.1002/adma.201502567.
- Song Z., C.L. McElvany, A.B. Phillips, I. Celik, P.W. Krantz, S.C. Watthage, G.K. Liyanage, D. Apul and M.J. Heben, "a techno-economic analysis of perovskite solar module

- manufacturing with low cost materials and techniques”, *Energy Env. Sci*, 2017,10, 1297-305, DOI:10.1039/C7EE00757D.
- Su B.B., G.J. Zhou, J.L. Huang, E.H. Song, A. Nag, and Z. G. Xia, "Mn<sup>2+</sup>-Doped Metal Halide Perovskites: Structure, Photoluminescence, and Application", *Laser Photonics Rev.* 2021, 15, 2000334, DOI: 10.1002/lpor.202000334.
- Vlaskin V. A., N. Janssen, J.V. Rijssel, R. Beaulac, D. R. Gamelin, "Tunable dual emission in doped semiconductor nanocrystals", *Nano Lett.* 2010, 10, 3670–3674, DOI:10.1021/nl102135k.
- Yan L., Q. Xue, M. Liu, Z. Zhu, J. Tian, Z. Li, Z. Chen, Z. Chen, H. Yan, H.-L. Yip and Y. Cao, "Interface Engineering for All-Inorganic CsPbI<sub>2</sub>Br Perovskite Solar Cells with Efficiency over 14%" *Adv. Mater.*, 2018, 30, 1802509, DOI:10.1002/adma.201802509.
- Zhang B.X., W.B. Bi, Y.J. Wu, C. Chen, H. Li, Z.L. Song, Q.L. Dai, L. Xu, and W. Song, "High-Performance CsPbI<sub>2</sub>Br<sub>2</sub> Perovskite Solar Cells: Effectively Promoted Crystal Growth by antisolvent and Organic Ion Strategies", *ACS Appl. Mater. Interfaces* 2019, 11, 33868–33878. <https://doi.org/10.1021/acsami.9b09171>.
- Zheng L.Q., G. Page and Z.R. Li, "ZnO nanowire embedded TiO<sub>2</sub> film as an electrode for perovskite CsPbI<sub>2</sub>Br solar cells", *RSC Adv.*, 2021, 11, 19705. <https://doi.org/10.1039/D1RA01563J>.